Development of a 3-D mammalian whole cell GFP-based assay system with high sensitivity and accuracy for drug discovery, biosensor, scale-down of large scale bioreactors and other biomedical applications

Xudong Zhang and Shang-Tian Yang*

Department of Chemical and Biomolecular Engineering, The Ohio State University, 140 West 19th Avenue, Columbus, Ohio 43210

*Corresponding author. Phone: (614) 292-6611. Fax: (614) 292-3769. Email address: Yang.15@osu.edu.

Abstract

Mammalian live cell fluorescent kinetic assays are always desired by the pharmaceutical industry, safety evaluation agencies and even basic science research because they are suitable for automatic high-throughput assay design and enable the characterization of rapid cellular events. However, fluorescent signals generated in such assays are usually too weak for in situ measurements. Three-dimensional (3-D) cell culture systems are better than 2-D cultures for efficacy analysis because 2-D culture models lack proper *in vivo* tissue functions and are inherently prone to error. We have designed, built and tested a simple 3-D whole cell GFP-based assay combining 3-D culture system into live cell fluorescent kinetic assay, which can increase the signal to noise ratio (SNR) at least one order of magnitude as compared to conventional 2-D cultures, and thus offers much more potential for biosensing systems using other sensing elements and reporters. In this 3-D system, embryonic stem cells with stable enhanced green fluorescent protein (GFP) expression were cultured on pre-treated nonwoven polyethylene terephpthalate (PET) fibrous scaffolds. The whole culture system was carried out in modified 96-well microplates stacked on a lab shaker in a cell culture incubator. A general fluorometer was used to quantify fluorescent intensity in real time. The effects of fetal bovine serum and fibronectin coating on 3-D ES cell culture were evaluated in the system. Embryocytotoxicity assays of dexamethasone (DM), diphenylhydantoin (DPH), penicillin G, and 5-fluorouracil (5-FU) and assays to monitor rapid cellular responses to Triton X-100 demonstrated the robustness of this new cell assay: enhancement of signal to noise ratio, elimination of labor intensive manual sample preparations, improvement of accuracy by 3-D culture superiority and minimization of errors due to biological system changes caused by cell activities. In addition, with the introduction of live cell kinetic assays instead of fixed endpoint assays, cytotoxicity can now be readily expressed upon a new standard: drug concentration to inhibit cell growth by 50% of the maximum growth rate. The results from this new 3-D system also showed differences in drug cytotoxicity responses as compared with those from the 2-D cell culture assays. The applications and advantages of this new potential high-throughput cell assay system in drug discovery, bioreactor process optimization, and the whole-process monitoring of embryonic stem cell differentiation are discussed in this paper.

Introduction

Drug discovery is a process involving biological target identification and validation, the selection of lead compounds for optimization, and clinical trials (Verkman et al, 2004). High-throughput screening plays an essential role in the initial identification of leads because the pool of chemical compounds and biological targets is rapidly expanding. After initial screening, compounds selected (hits) are evaluated for many criteria, including efficacy and toxicity to identify leads. In this step, cell viability and proliferation assays in cell culture models are always applied. Currently, pharmaceutical firms spend much money on the compound efficacy and cytotoxicity test than in any other area. (DiMasi et al., 2003). However, 22.5% of compounds still fail during testing, which may be devastating to developing companies. Effective compounds in vitro may be null in vivo for many reasons, including differences between in vitro and in vivo target biology, poor penetration into solid tissues, et al. Currently, almost all cell based assays or biosensors are developed in 2-D culture systems, while conventional 2-D cultures usually suffer from contact inhibition and a loss of native cell morphology and functionality. In comparison with 2-D cultures, cells in 3-D cultures mimic the in vivo situation more closely, which is critical to many important cell functions, including morphogenesis, cell metabolism, gene expression, differentiation and cell-cell interactions (Mueller-Klieser et al, 1997). Therefore, discrepancies in predicted drug treatment effectiveness in 2-D and 3-D cultures describe the advantage of using 3-D culture systems (Kobayashi et al, 1993). For cell-based sensing, particularly in studying cytotoxicity and drug discovery, maintaining the cell in its native functional state in a proper 3-D environment would improve predictions and have the potential to reduce clinical trial failures. However, despite the higher efficacy of cell assays that can be obtained by using 3-D culture systems, so far, few cell sensors based on these in vivo-like tissue models have been developed due to the complexity of 3-D cultures. Fibrous materials, such as nonwoven polyethylene terephthalate (PET), are shown to be advantageous 3-D scaffolds to immobilize cells because of their high specific surface areas, mechanical properties, and void volume in addition to easy manipulation, and may be the proper matrix material to exploit the advantages of 3-D systems in cell assays and biosensors (Li et al., 2001).

Results

Correlation between fluorescent signal and the cell number

A linear correlation of fluorescent signals and cell numbers was found for all cell concentrations tested when cells were suspending in PBS (Figure 2A) or on 3-D PET scaffolds (figure 2B). This matches the results of Hunt et al, 1999 that the layering of cells does not significantly impair signal detection. The fact that the slope of Figure 2B was about 3 times larger than that of Figure 2A was not expected by the authors. Repeated experiments showed similar results. One possibility was that 6 hours' recovery of fluorescence caused much higher cell specific fluorescence in Figure 2B. However, the fact that even with 6 hours of recovery after inoculation the slope of the curve for cells in medium was only a little larger than that in Figure 2A and much less than that in Figure 2B indicated that there were other factors involved. The most probable assumption was that the optical combination of fluorescence from the

EGFP proteins and PET fibers can enhance fluorescent signals several times.

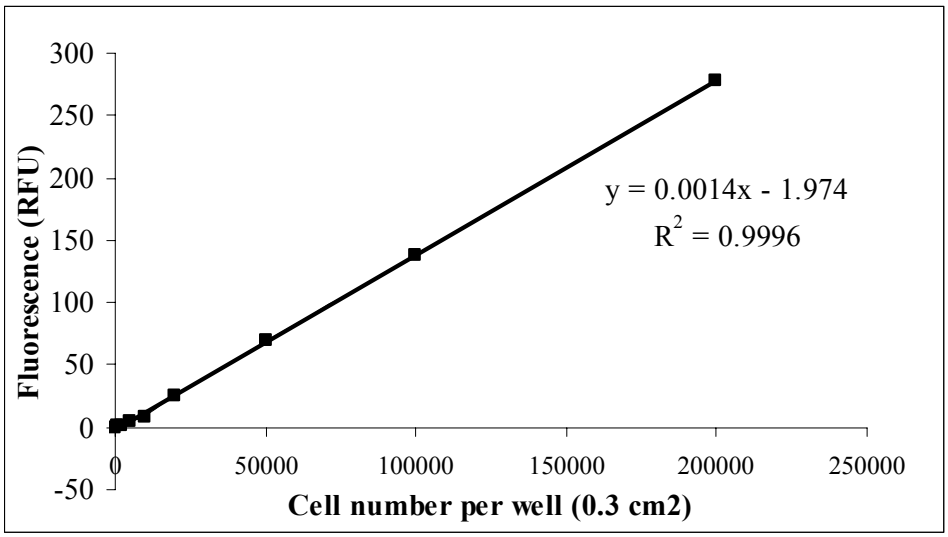

A

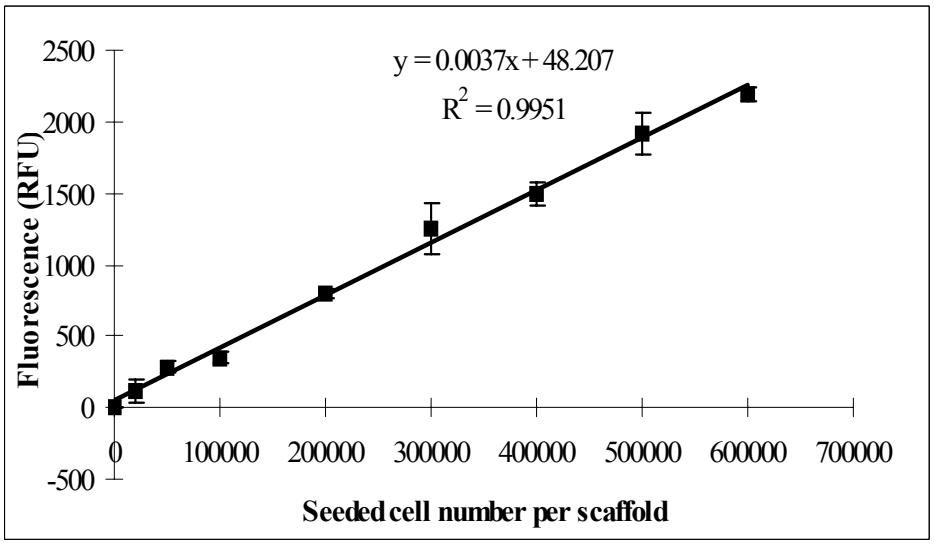

B

Figure 2. Fluorescent intensity is proportional to cell number either in PBS suspension or on 3-D scaffolds. **A.** In PBS suspension. Cell number was from 10^3 to $2*10^5$ cells/well. Each point represents the average fluorescent intensity from triplicate samples minus average intensity of the PBS blanks, which are about 60 RFU. **B.** On 3-D scaffolds. Each point represents the average fluorescent intensity from triplicate samples minus average intensity of the blanks. The blanks consist of fluorescent signals from medium and scaffolds, which is totally about 700 RFU.

2-D fluorescent kinetics of cell growth

For ES-GFP cells, a large discrepancy existed between the fluorescence given by live cells

and the total fluorescence, especially when the fluorescent signals were high (Figure 3). The discrepancy between the total fluorescence and the fluorescence from the live cells for the wild-type (wt) ES lineage was only a little less than that for the ES-GFP lineage at 146 h after inoculation. This indicated that in addition to GFP released from dead cells, changes in the medium components caused by cell activities and cell debris contributed most of the fluorescent discrepancy between the live cell fluorescence and the total fluorescence for the ES-GFP lineage. This is inconsistent with the suggestion from Girard et al, 2001 that only the stability of GFP released into the medium contributed the discrepancy between the total fluorescence and the viable cell number. In addition, there was a 13 hour interval between the time points for the maximum live cell fluorescence and the maximum total fluorescence. The significant differences with or without medium replacement suggested that the total fluorescence could not be applied to in situ quantification of cell numbers unless the errors caused by cell culture medium component changes, cell debris and GFP released from dead cells were eliminated.

We should also notice that fluorescent compounds in the medium, which were susceptive to natural light, elicited an approximately 500 RFU background signal, more than 2 times the maximal signal given by live cells. Therefore, the removal of medium before each measurement is necessary to improve the accuracy for the 2-D culture quantification.

Therefore, the fluorescence from live cells instead of the total fluorescence was used for later cytotoxicity tests in 2-D system.

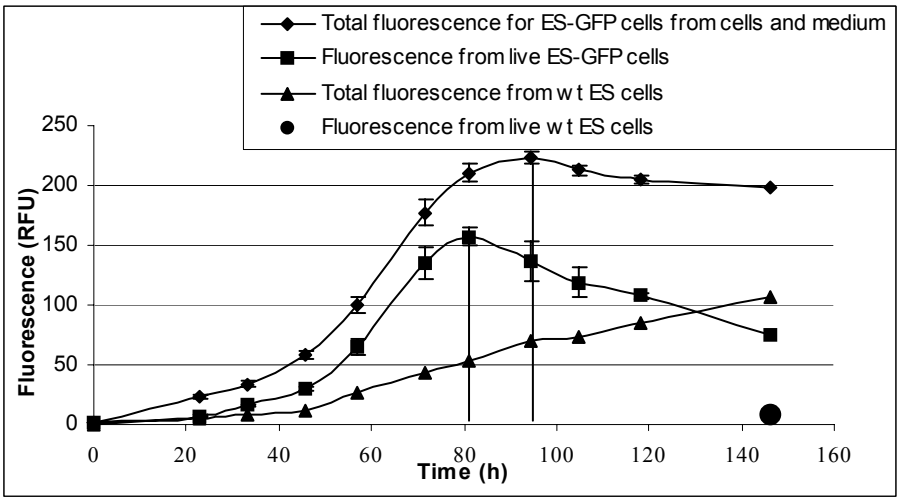

Figure 3. Difference between the total fluorescence and the fluorescence given by live cells for the ES-GFP lineage and the wt ES lineage. In the first two curves, each point represents the average fluorescent intensity from triplicate samples minus the average intensity of the medium or PBS blanks. In the third curve, each point represents the fluorescent intensity only from one sample minus average intensity of the PBS blanks.

Quantification of 3-D cell growth kinetics

25 000 cells in 25 µl medium were inoculated into each scaffold (Figure 4A). The fluorescence

of the live cells in our system was calculated using Eq. (2):

$$F_{cells}=F_{center}-F_{scaffold}-F_{surround} \quad (2)$$

$F_{scaffold}$ represents the fluorescent signal of a scaffold soaked in PBS, a constant during the entire culture process. F_{center} represents the fluorescent signal measured from the central well in which a scaffold with growing cells has been fixed. $F_{surround}$ represents the average fluorescent signal measured from 8 wells surrounding the central well. F_{center} and $F_{surround}$ can be obtained directly by taking fluorescence measurements twice per day.

In the semi-log plot (Figure 4B), the slopes of the growth curves from 50 h to 90 h after inoculation (the exponential phase of cell growth) represent the maximum growth rates. The average of these three maximum growth rates was calculated to be 0.0035 h^{-1}(doubling time 20 h) (all R^2>0.999).

Our 3-D growth curves (Figure 4A) had a similar stationary phase to the live cell fluorescent growth curve in Figure 3, which was much shorter than the total fluorescent growth curve in Figure 3 and the growth curve from Hunt el al, 1999. This indicated that errors caused by medium component changes, cell debris and released GFP were almost removed, if not thoroughly eliminated. Therefore, higher accuracy was achieved because our system could minimize these errors automatically, which was much more crucial for cytotoxicity assays.

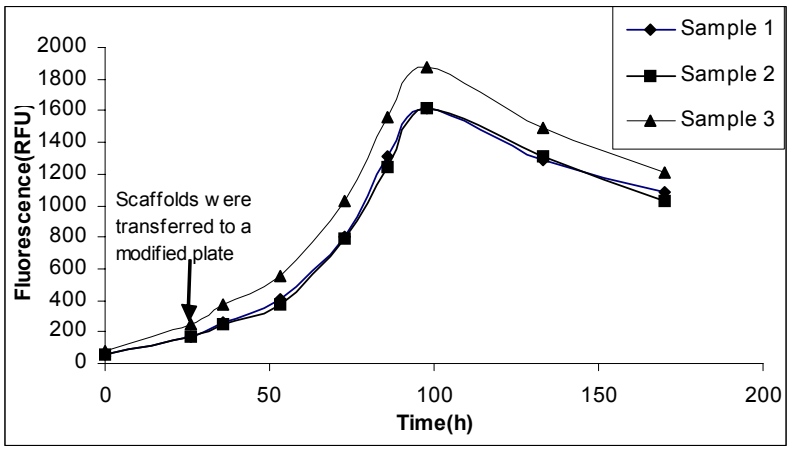

A

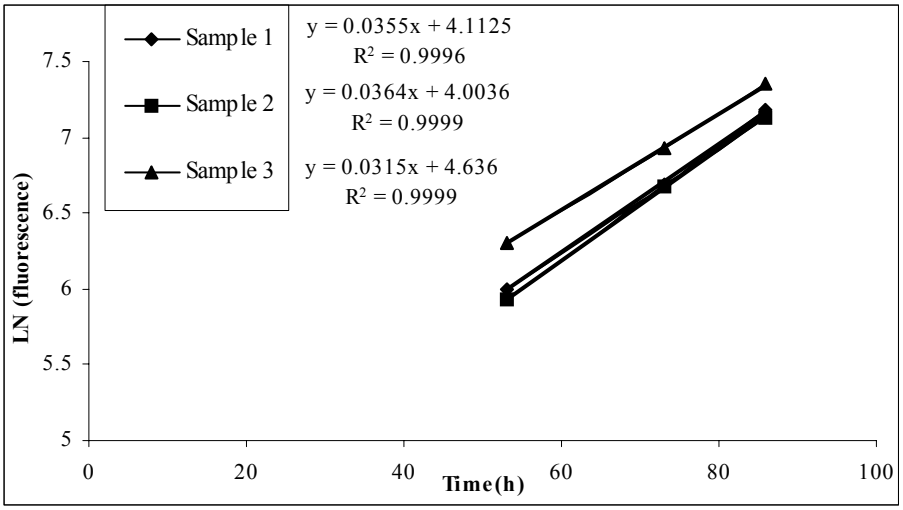

B

Figure 4. Quantification of cell growth kinetics by fluorescent signals. **A.** Fluorescence kinetics during cell growth. Each curve represented fluorescent changes for one sample. All of these samples were in the same modified plate. **B.** Semi-log plot of fluorescence kinetics during cell growth. The exponential phase of cell growth was used to calculate the maximum cell growth rate (μ_m). μ_m of 3 samples are 0.0355, 0.0364, 0.0315 h^{-1} respectively.

Optimization of culture system: evaluation of effects of serum concentration and fibronectin coating

The increase of growth rate between 0% and 1% FBS was significant (Figure 5), but not much influence was found above 1%. Therefore, 1% FBS is probably enough to economically support cell growth in industrial production of the 3-D culture system.

Fibronectin is involved in many cellular processes, one of which is serving as a general cell adhesion molecule to help cells anchor to proteoglycan or collagen substrates. (Yamada et al, 1992). As shown in Figure 6, fibronectin coating conferred a distinct enhancement to the maximum cell growth rate (μ_m). With fibronectin coating, Um increased from 0.0032 h^{-1} to 0.0043 h^{-1}, a 35% enhancement. When the cell culture with fibronectin coating reached the maximum fluorescent intensity (128 h after inoculation), the fluorescent intensity with fibronectin coating was 2.5 times of that without fibronectin coating. This enhancement could be because uniform distribution benefited the mass transfer and improved in- or out gassing so that cells lived in a constant pH environment with a supply of nutrients and oxygen and the removal of metabolites. Pictures (Figure 7A, 7B) from a fluorescent microscope (Nikon Ecllipse TE2000-U) indicated that the fibronectin coating benefited cell adherence to PET fibers. In addition, cells with fibronectin coating were distributed more uniformly along the fibers, while those without fibronectin coating formed larger aggregates (Figure 7C, 7D).

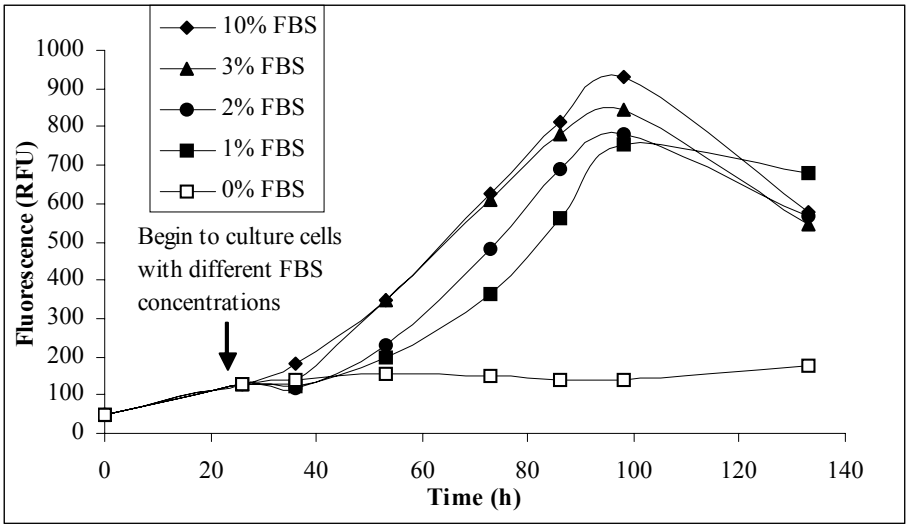

Figure 5. Effect of serum on cell growth.

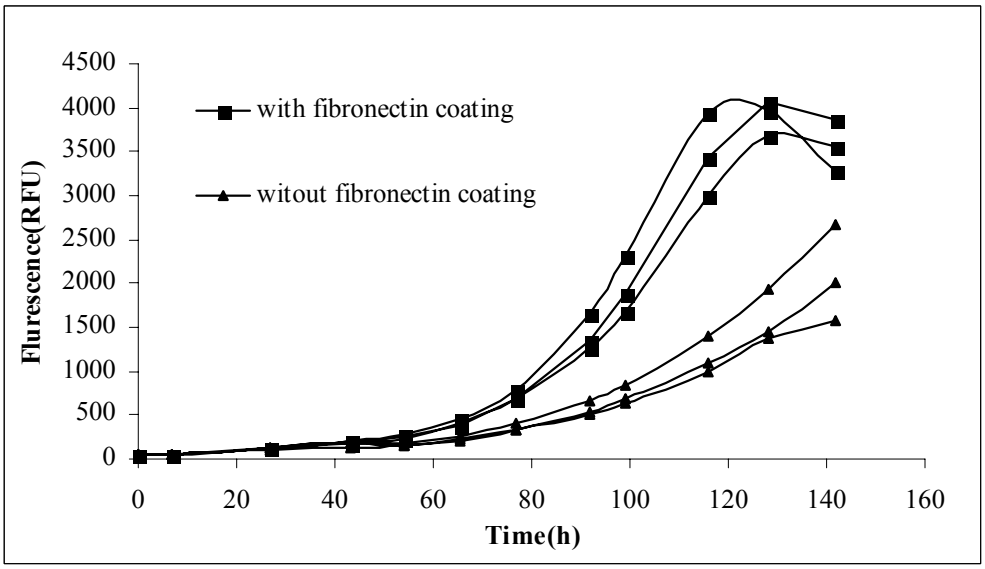

Figure 6. Fibronectin coating enhanced cell growth. Three samples were with fibronectin coating, while the other three samples were without fibronectin coating. Each curve represented changes of fluorescent intensity for each sample over time. All of these 6 samples were in the same modified plate.

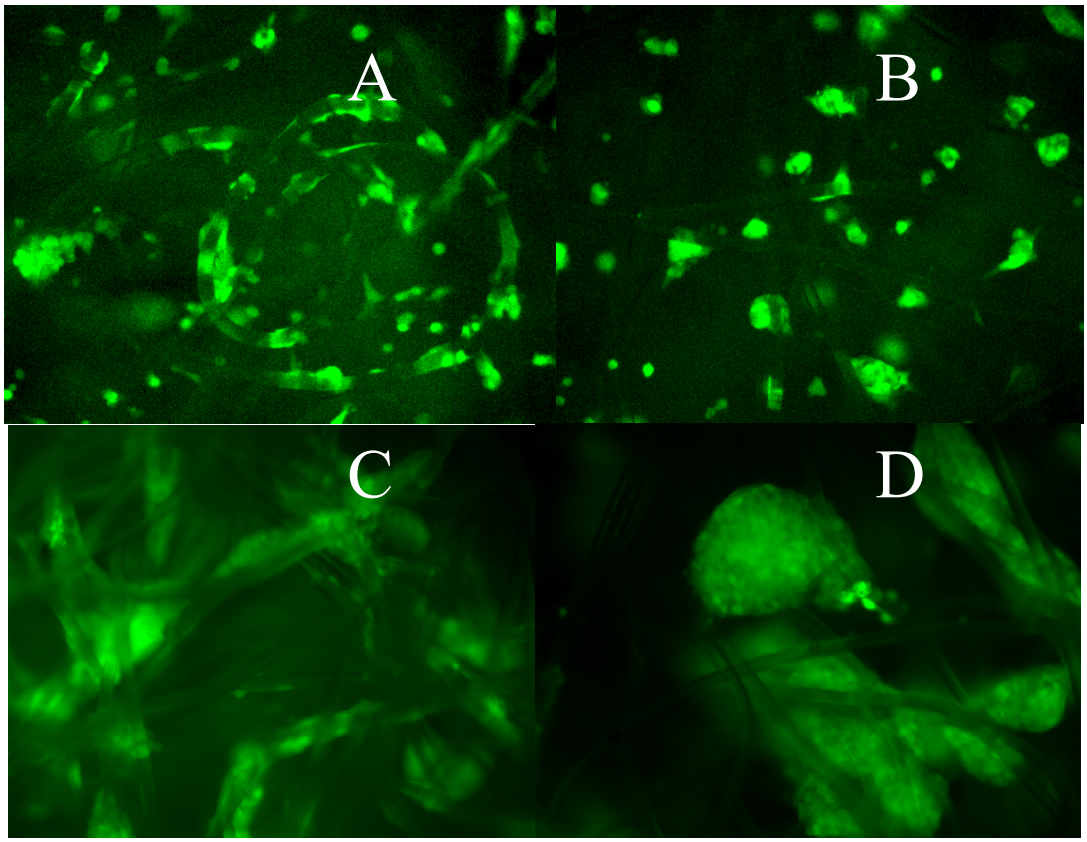

Figure 7. Fluorescent microscopic images of ES-GFP cells on 3-D scaffolds. A. one day after inoculation with fibronectin coating; B. one day after inoculation without fibronectin coating; C. 3 days after inoculation with fibronectin coating; D. 3 days after inoculation without fibronectin coating. An inverted fluorescent microscope (Nikon Ecllipse TE2000-U) was used for detection.

Cytotoxicity studies

To demonstrate the feasibility of our system for toxicological study, cells on 3-D scaffolds were exposed to four embryotoxic reference substances: DM, DPH, penicilliin G and 5-FU. Cytotoxicity in our 3-D system was expressed as the concentration of analytes causing 50% inhibition of the cell maximal growth rate ($I\mu_{m50}$).

The fluorescent kinetics with different concentrations of DM is shown in Figure 8A. The maximum cell growth rate decreased as the concentration of DM increased. The maximum growth rate for each DM concentration was calculated using the exponential growth phase from 51.5 h to 111.5 h after inoculation. Figure 8B shows the correlation between DM concentrations and maximal growth rates in 3-D (all R^2>0.99, when μ_m were calculated) and in 2-D. $I\mu_{m50}$ of DM were 11.5 μg/ml in the 3-D system and 32 μg/ml in 2-D system, according to these curves. Another repeated experiment showed $I\mu_{m50}$ was 13.5 μg/ml in 3-D system (Figure 8C). $I\mu_{m50}$ of DPH in 3-D and 2-D were 39 μg/ml and 30 μg/ml; $I\mu_{m50}$ of Penicillin G in 3-D and 2-D were 750 μg/ml and 4500 μg/ml; $I\mu_{m50}$ of 5-FU in 3-D and 2-D and 0.035 μg/ml and 0.045 μg/ml. (Figure 9, Figure 10, Figure 11).

All the cytotoxicity test results for these four drugs in our 2-D and 3-D systems were compared to the results from Scholz et al, 1999 (Table 1). All cytotoxicity values in 3-D are lower than those in 2-D and the results from Scholz et al, 1999, except for DPH. For DM and Penicillin G, $I\mu_{m50}$ in 3-D are 3 and 6 times of $I\mu_{m50}$ in 2-D, respectively, which is close to the results from Scholz et al, 1999. The difference of 5-FU cytotoxicity in 3-D and 2-D is not significant. $I\mu_{m50}$ of DHP in 2-D is similar to 3-D, which is lower than the results from Scholz et al, 1999. We also noticed that in the 2-D system, DPH formed crystals on the bottom of wells. The higher the concentration, the more crystals formed. This might lead to a stronger effect on cells attaching to the bottom in 2-D culture. On the other hand, in our 3-D culture system, there were very few crystals formed due to continuous agitation. The fact that $I\mu_{m50}$ of DPH in 2-D was even lower than that in 3-D, which is not like the other three drugs, partly confirmed the assumption that chemicals with low dissolvability have a stronger effect in static 2-D cultures due to the formation of crystals, while agitation in 3-D culture can help dissolve chemicals, mimicking the *in vivo* situation.

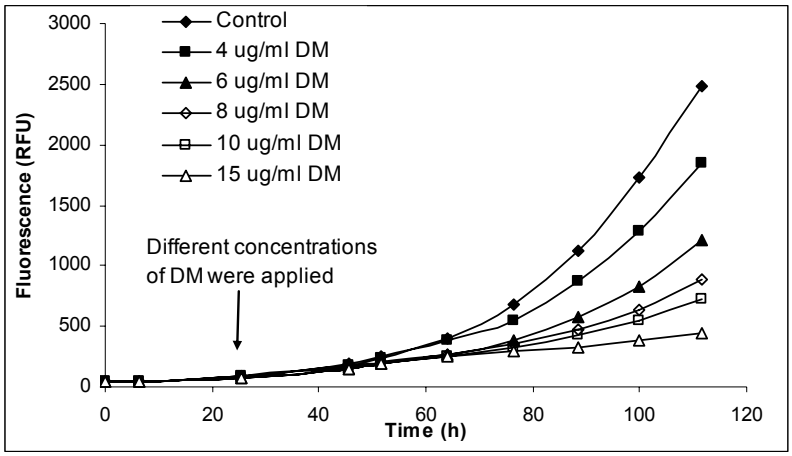

A.

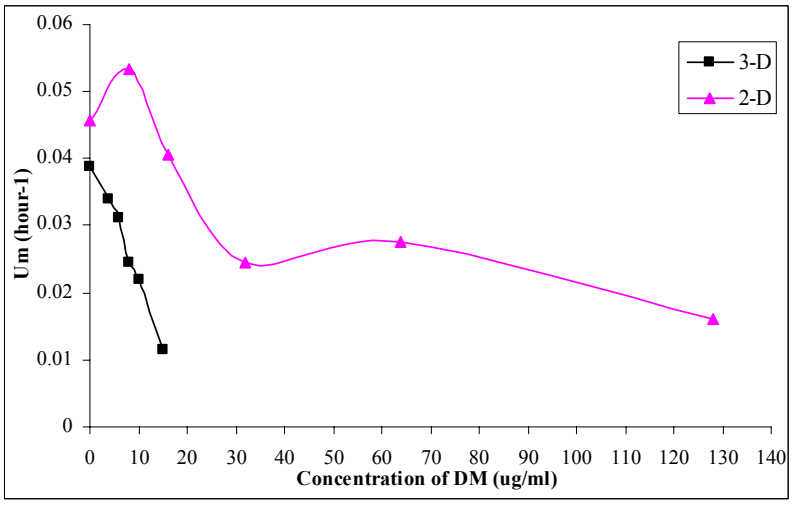

B.

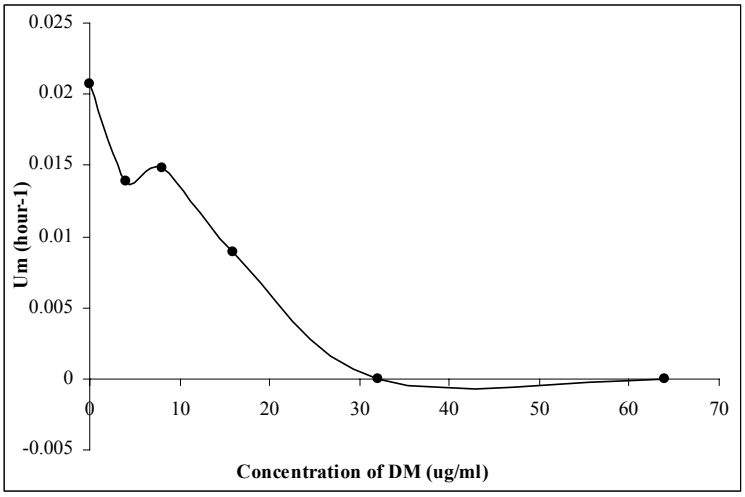

C.

Figure 8. Embryocytotoxicity of DM in 3-D and 2-D system. **A.** ES-GFP cell fluorescence kinetics with different DM concentrations. **B.** Correlation between DM conc. and Um in 3-D system and 2-D system. As the DM conc. increased, μ_m decreased. The cytotoxicity of DM was expressed as the DM conc. causing 50% inhibition of μ_m. Iμ_{m50} of DM in 3-D and 2-D were 11.5 μg/ml and 32 μg/ml according to these two curves. **C.** Repeated experiment showed IUm_{50} of DM was 13.5 μg/ml in 3-D system.

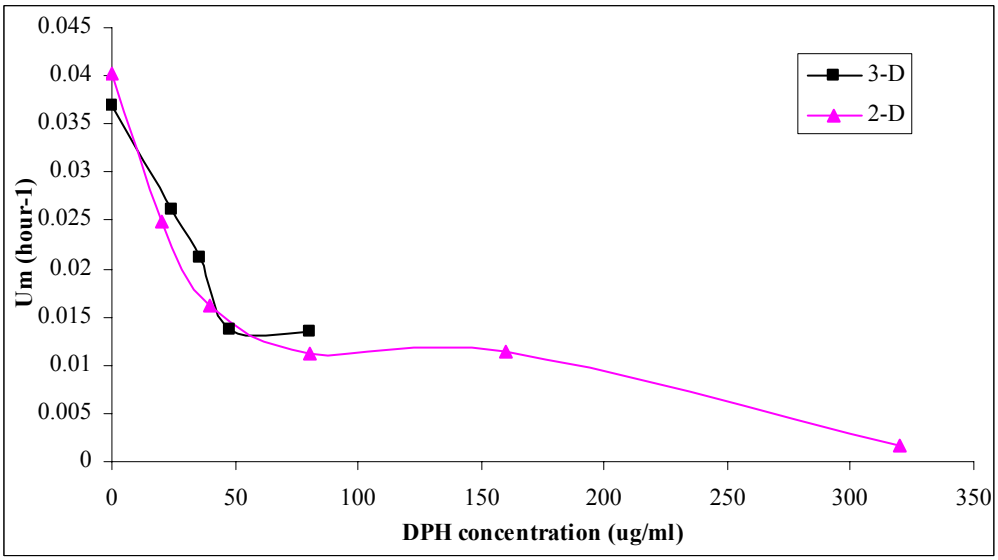

Figure 9. Correlation between DPH conc. and Um in 3-D system and 2-D system. Iμ_{m50} of DPH in 3-D and 2-D were 39 μg/ml and 30 μg/ml according to these two curves.

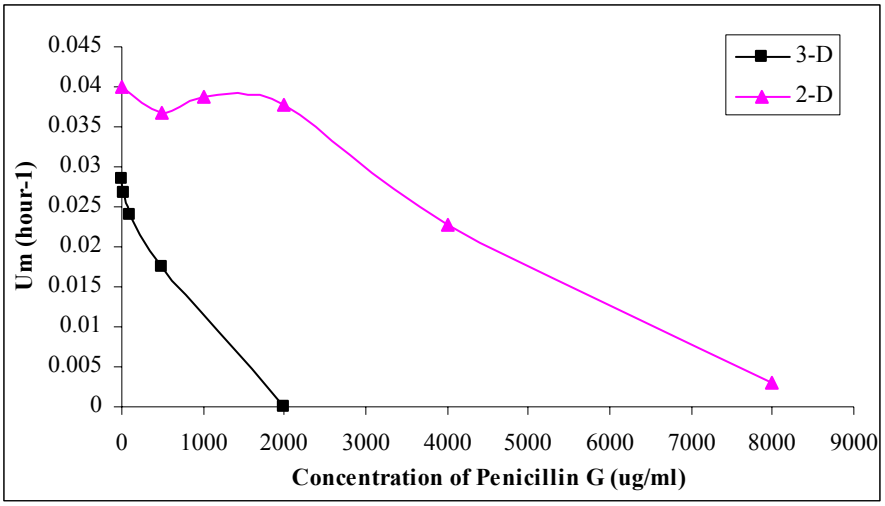

Figure10. Correlation between Penicillin G conc. and Um in 3-D system. IUm_{50} of Penicillin G in 3-D and 2-D were 750 µg/ml and 4500 µg/ml according to these two curves.

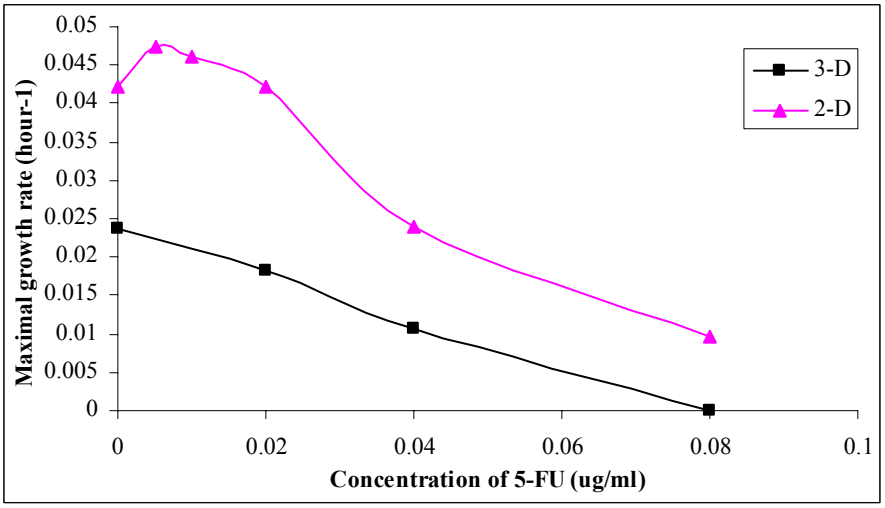

Figure 11. Correlation between 5-FU conc. and Um. ; $I\mu_{m50}$ of 5-FU in 3-D and 2-D and 0.035 µg/ml and 0.045 µg/ml according to these curves.

Table 1. Comparison of cytotoxicity test results in 2-D and 3-D with different cytotoxicity expressions

	Dexamethasone(weak embryocytotoxicity)	Penicillin G(non-embryocytotoxocity)	Diphenylhydantoin(weak embryocytotoxicity)	5-fluorouracil (strong embryocytotoxicity)
3-D system ($I\mu_{m50}$)	11.5 µg/ml	750 µg/ml	39 µg/ml	0.035 µg/ml
2-D system ($I\mu_{m50}$)	32 µg/ml	4500 µg/ml	30 µg/ml	0.045 µg/ml
ZEBET $IC_{50}D_3$ (phase III testing, Scholz G et al, 1999)	37 µg/ml	2100 µg/ml	102 µg/ml	0.09 µg/ml
ECVAM $IC_{50}D_3$ (phase III testing, Scholz G et al, 1999)	51 µg/ml	2000 µg/ml	195 µg/ml	0.065 µg/ml

ZEBET (Center for Documentation and Evaluation of Alternative Methods to Animal Experiments), ECVAM (European Centre for the Validation of Alternative Methods) were two institutes involved in the EST.

Assessment of rapid cellular events

Because online continuous measurements can be made with no human attention required in live-cell kinetic assays, rapid cellular events can be readily characterized. Figure 12 shows the acute toxicity of Triton X-100. Triton X-100 is a non-ionic detergent commonly used to solubilize membrane proteins. The slow decrease of the fluorescent signal in the control might be due to an increase of environmental pH from the cell culture incubator to the plate carrier of the fluorometer, which affected the fluorescent components in the whole culture system.

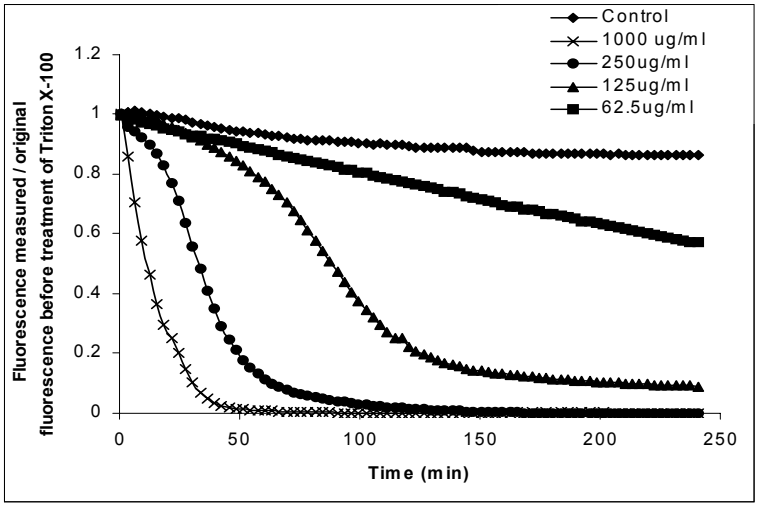

Figure 12. Acute cellular responses to Triton X-100. Different curves represent acute cell responses to different Triton X-100 concentrations.

Discussion

Process optimization for 3-D adhesive mammalian cell cultures such as the Fibrous Bedded Bioreactor (Yang et al, 2004) in spinner flasks, is less practical due to time-consuming, high expense and lack of parallelity. In addition, frequent sampling also contributes to the risk of contamination. Although static experiments can be conducted in parallel, reducing labor and cost, static microplate cultures are not able to confer enough agitation to support 3-D cell cultures with high cell densities. Our 3-D system overcomes most of these limitations. Because it enables the monitoring of cell growth kinetics on line in real time automatically and parallely, the system can serve as a very powerful tool for scale-down, providing crucial information for the bioprocess refinement of bench or pilot systems. According to the results above, applying fibronectin coating, large scale designs may achieve a much higher efficiency due to the increase in the growth rate and the maximum cell density.

The determination of signals correlated to cell responses is fundamental, no matter what principle of a cell-based assay or a biosensor is used. Thus, signal to noise ratio (SNR) is one essential criterion to evaluate an assay or sensor. Compared with 2-D cultures, our 3-D system has an extra 180-240 RFU background fluorescent signal because of the PET scaffolds. However, for each sample, the background fluorescent signal caused by the scaffold was a constant throughout the entire experiment process, unlike culture medium which is susceptible to light. Therefore, the experimental noises of 3-D are close to that of 2-D. On the other hand, the maximum fluorescent signal given by our 3-D culture can be higher than 5000 RFU, while the maximum fluorescent signal in 2-D is less than 250 RFU for the same ES-GFP cell line. Therefore, our 3-D system increases SNR at least one order of magnitude compared with 2-D cultures. We should also notice that CMV is a strong constitutive transcription activator which is much stronger than most cis-acting genetic elements corresponding to specific functional units. In addition, EGFP is also a strong autofluorescent protein. Therefore, in standard 2-D cultures, resulting signals are weak compared to background noises, as our results show, even with the combination of these two strong factors, so fluorescence quantification would fail due to low SNR when other genetic elements or other autofluorescent proteins were applied. In this context, our 3-D system might provide a solution.

The exact signals representing cell responses are another point which must be considered for any cellular assay or biosensor. The stability of autofluorescence from released GFP, cell debris and fluorescent fluctuation of medium due to cell activities or environment changes were other defects preventing the popularity of live-cell GFP fluorescent assays. It becomes a more critical issue for cytotoxicity studies in which cell death is one of the foci. In our 3-D system, the fluorescence from live cells are all centralized in the center well (about 0.3 cm^2) and the background fluorescence is uniformly distributed in the whole culture area (about 9 cm^2) due to agitation. Therefore, theoretically, the errors caused by released GFP, cell debris and fluorescent fluctuation of medium are about 1/30 that of standard 2-D culture systems, if fluorescent signals from central wells are considered as live cell fluorescent signals. Actually, in all of our data we used Eq. (2) to calculate live cell fluorescence, so it is possible that these errors are further reduced. Because of the convergence of resulting fluorescent signals, both signal magnitude and accuracy are highly improved in our 3-D system. At this point, our system can serve as a very good prototype of cellular assays and biosensors.

Recently, we discovered that cow luteal cells cultured in a 3-D environment were able to maintain their in vivo function for a longer period than cells cultured in 2-D. The ability for cells to maintain their normal functions and responses to environmental stimuli is critical in the development of cell-based biosensors with portability for field and point-of-care use applications. In addition, 3-D culture could also enable a sensor to test the cytotoxicity of those analytes requiring a longer period to take effect. On the other hand, as the above results show, because our system allows the realization of live-cell kinetic assays that avoid the need for sample preparation, enzyme reactions, and antibody development, it can provide information regarding rapid cellular events, which is not easily detected by fixed endpoint assay methods but is always desired by biosensors.

In EST, cytotoxicity was expressed as the drug concentration causing 50% inhibition of cell number at a certain time point ($IC_{50}D_3$). Because cell number ratios of drug-treated samples to the control varied from time to time, the values of cytotoxicity with this expression varied according to the different time points chosen. Thus, it cannot provide an invariable standard for cytotoxicity tests, especially when different cell lines have different growth rates. In this context, the concentration of an analyte inhibiting the cell maximal growth rate by 50% of the control level could be a better choice because the maximal growth rate is only determined by the cell line used and culture conditions such as medium components, pH, agitation rate, and the concentrations of analytes. For a certain biological system, it is a constant instead of a variable. However, application of this expression for large scale cytotoxicity screening would create an undaunted work load with conventional counting methods. Our real-time system eliminated all cumbersome steps in manual sample preparation or enzyme reaction for counting and readily enabled the application of this new expression. At this point, it could be a better cell-based assay for the cytotoxicity test of chemical compounds and environmental factors.

In our current system, plates were fabricated by a general drill, so the uniformity of incision was low. Accuracy might be increased if advanced fabricating instruments such as a Computer Numerical Controlled (CNC) machine or other microfabrication machines could be applied to obtain a higher uniformity of incision. In addition, because it took us a long time to fabricate a plate, modified plates had to be recycled to achieve all the data in this paper. This led to certain chances of contamination and variances of background fluorescence due to abrasion. If our system was commercialized, the very low unit cost of these modified plates, due to mass-production, would allow them to be disposable. Therefore, both the qualification and efficiency of the system would dramatically improve.

Simplicity is necessary for an assay or sensor adapted to routine lab use. In our system, the online quantification of autofluorescent signals can be realized simply with PET scaffolds, a modified 96-well plate, a standard bench shaker, and a general fluorometer in addition to regular cell culture materials. For manipulation, our system has additional requirements for scaffold treatment and plate modification compared to 2-D systems. (Recent experiments showed that transferring scaffolds was not necessary, since cells unattached to the scaffolds contributed less than 5% of the total fluorescent intensity.) However, since PET is a durable material, scaffolds can be prepared and treated in large quantity and stored for a long period of time (several months). The ease of both plate fabrication and scaffold pretreatment would make the system ready for mass production if it is commercialized. We can imagine that when modified plates in which treated scaffolds were prefixed were commercialized, the entire experiment setup would only include cell inoculation and the addition of analyte-containing

medium. In addition, installation of the detection part of a fluorometer in a cell culture incubator would allow us to conduct assays without any user attention after initiation.

Assessment of high-throughput screening (HTS) is taking on a new role with great significance when the pool of chemical compounds and biological targets are expanding rapidly. Although our system, limited by the fabrication technique, currently only allows 6 samples in one plate, we believe that it can be amenable to high-throughput experiments by processing many small-scale bioreactors in parallel when applying microfabrication techniques. Further optimization of microplate configuration and sealing technology to avoid contamination will also improve the performance of our system.

Because most of the differentiation processes require ES cells to form aggregates such as EBs and then simultaneously develop into various cell phenotypes, an *in vitro* assay with wide type ES cells for the quantitative assessment during development processes is complicated. Normally, immunological or molecular methods are required to quantify specific cell types. These are time-consuming and therefore not suitable for the design of automated, high-throughput screening cell assays and kinetic studies of the entire differentiation process. Because cell layering did not impair significantly signal detection using a fluorometer (Hunt et al, 1999), our 3-D system would stand many chances to monitor full-scall differentiation to specific lineages in EBs when CMV was replaced by a tissue restricted promoter as Bremer et al, 2001; Paparella et al, 2002 did. In addition to 3-D ES cell differentiation, other engineered cell lineages containing reporter genes coupled to particular biological recognition components can be applied in order to study other 3-D tissue models. Our work addresses a prototype for advanced future 3-D cell culture arrays.

Cell number or cell mass quantification is still an issue preventing the further development of 3-D tissue engineering. Using an indirect way to automatically quantify, our system can provide a simple but efficient platform to explore the benefit of 3-D tissue engineering. In this paper, the optimization of 3-D cultures and a simple comparison of the different cytotoxicities of drugs in 2-D and 3-D were made. Further attempts to discern different drug performance on different tissue models are now being conducted. In addition, with different fluorescent proteins applied at the same time, the automatic monitoring of co-cultured tissue models will also be realized.

Conclusion

Our system offers an *in vivo* mimic, convenient, automatic, on line in real-time, high-throughput potential method for quantifying cell numbers or cell mass. It potentially offers a platform for application to many different disciplines including high-throughput screening of novel drugs, potable cell based sensors, bioreactor optimization, and basic biomedical research such as functional genetics, systems biology, and quantitative cell biology. Compared to currently used live-cell autofluorescent assays, our 3-D system has five advantages. Firstly, the reliability is improved because cells in 3-D culture have more desired functional attributes representing the in vivo native counterparts. Secondly, the fact that our 3-D culture system can enhance signals by 20 folds compared with 2-D culture system means a higher sensitivity and enables much more applicability for on-line automation using other biological recognition components and fluorescent proteins. Thirdly, higher accuracy is achieved because unnegligible errors due to cell activities are almost completely eliminated by the convergence of resulting signals and the uniform distribution of background signals. Fourthly, the elimination of sample preparation for

counting makes the constant expression of cytotoxicity ready and gives more chances to monitor cellular rapid events. Finally, the simple design as mentioned above offers high adaptability for routine lab cell assays. Currently, an optimal combination of these five attributes is unmatched by any other cell assay or biosensor found by the authors.

Reference

Ashcroft RG, Lopez PA. 2000. Commercial high speed machines open new opportunities in high-throughput flow cytometry (HTFC). J Immunol Methods 243:13-24.

Bremer S, Worth AP, Paparella M, Bigot K, Kolossov E, Fleischmann BK, Hescheler J, Balls M. 2001. Establishment of an in vitro reporter gene assay for developmental cardiac toxicity. Toxicol In Vitro 15:215-23.

Daunert S, Barrett G, Feliciano JS, Shetty RS, Shrestha S, Smith-Spencer W. 2000. Genetically Engineered Whole-Cell Sensing Systems: Coupling Biological Recognition with Reporter Genes. Chemical Reviews (Washington, D. C.) 100:2705-2738.

DiMasi Joseph A; Hansen Ronald W; Grabowski Henry G. 2003. The price of innovation: new estimates of drug development costs. Journal of health economics 22:151-85.

Gerrard L, Zhao D, Clark AJ, Cui W. 2005. Stably Transfected Human Embryonic Stem Cell Clones Express OCT4-Specific Green Fluorescent Protein and Maintain Self-Renewal and Pluripotency. Stem Cells 23:124-33.

Gorba T, Allsopp TE. 2003. Pharmacological potential of embryonic stem cells. Pharmacol Res 47:269-78.

Hunt L, Batard P, Jordan M, Wurm FM. 2002. Fluorescent proteins in animal cells for process development: optimization of sodium butyrate treatment as an example. Biotechnol Bioeng 77:528-37.

Hunt, L.; Jordan, M.; De Jesus, M.; Wurm, F. M. 1999. GFP-expressing mammalian cells for fast, sensitive, noninvasive cell growth assessment in a kinetic mode. Biotechnology and Bioengineering 65: 01-205.

Kobayashi, H., S. Man, C. H. Graham, S. J. Kapitain, B. A. Teicher, and R. S. Kerbel. 1993. Acquired multicellular-mediated resistance to alkylating agents in cancer. *Proc. Natl. Acad. Sci. USA* 90: 3294–3298.

Li Y; Ma T; Kniss D A; Yang S T; Lasky L C. 2001. Human cord cell hematopoiesis in three-dimensional nonwoven fibrous matrices: in vitro simulation of the marrow microenvironment. Journal of hematotherapy & stem cell research 10:355-68.

Mueller-Klieser W. 1997. Three-dimensional cell cultures: from molecular mechanisms to clinical applications. American Journal of Physiology 273:C1109-C1123.

Paparella M, Kolossov E, Fleischmann B. K, Hescheler J, Bremer S. 2002. The use of quantitative image analysis in the assessment of in vitro embryotoxicity endpoints based on a novel embryonic stem cell clone with endoderm-related GFP expression. Toxicology in Vitro 16:589-597

Ramirez S, Aiken CT, Andrzejewski B, Sklar LA, Edwards BS. 2003. High-throughput flow cytometry: validation in microvolume bioassays. Cytometry A 53:55-65.

Scholz G, Genschow E, Pohl I, Bremer S, Paparella M, Raabe H, Southee J, Spielmann H. 1999. Prevalidation of the embryonic stem cell test (EST) - a new in vitro embryotoxicity test. Toxicology in Vitro 13:675-681.

Verkman AS. 2004. Drug discovery in academia. American Journal of Physiology 286:C465-C474.

Yamada KM, Aota S. Akiyama SK, LaFlamme SE. 1992. Mechanisms of fibronectin and integrin function during cell adhesion and migration. Cold Spring Harbor Symposia on Quantitative Biology 57:203-12.

Yang ST, Luo J, Chen C. 2004. A fibrous-bed bioreactor for continuous production of monoclonal antibody by hybridoma. Adv Biochem Eng Biotechnol 87:61-96.